# Band structure engineering of semiconductors for enhanced photoelectrochemical water splitting: The case of $TiO_2$

Wan-Jian Yin, Houwen Tang, Su-Huai Wei, Mowafak M. Al-Jassim, John Turner, and Yanfa Yan*
*National Renewable Energy Laboratory, Golden, Colorado 80401, USA*
(Received 20 April 2010; revised manuscript received 12 May 2010; published 12 July 2010)

Here, we propose general strategies for the rational design of semiconductors to simultaneously meet all of the requirements for a high-efficiency, solar-driven photoelectrochemical (PEC) water-splitting device. As a case study, we apply our strategies for engineering the popular semiconductor, anatase $TiO_2$. Previous attempts to modify known semiconductors such as $TiO_2$ have often focused on a particular individual criterion such as band gap, neglecting the possible detrimental consequence to other important criteria. Density-functional theory calculations reveal that with appropriate donor-acceptor coincorporation alloys with anatase $TiO_2$ hold great potential to satisfy all of the criteria for a viable PEC device. We predict that (Mo, 2N) and (W, 2N) are the best donor-acceptor combinations in the low-alloy concentration regime whereas (Nb, N) and (Ta, N) are the best choice of donor-acceptor pairs in the high-alloy concentration regime.

DOI: 10.1103/PhysRevB.82.045106 PACS number(s): 71.20.Nr, 61.72.Bb, 71.55.Ht, 84.60.−h

## I. INTRODUCTION

The search for new semiconducting materials and/or the engineering of existing semiconductors for commercially viable photoelectrochemical (PEC) water splitting has been extremely challenging. Meeting that challenge requires the discovery of a semiconductor with the following tightly coupled material property criteria: appropriate band gap (1.6–2.2 eV), efficient visible light absorption, high carrier mobility, and correct band-edge positions that straddle the water redox potentials. Trial-and-error synthesis approaches have proven ineffective in discovering a viable material. As an example, anatase $TiO_2$ is one of the most studied materials owing to its good photocatalytic activity, ease of synthesis, long-term chemical stability, and demonstrated PEC applications.[1–3] However, its large band gap (~3.2 eV) fails to absorb a significant fraction of visible light, resulting in poor solar-to-hydrogen conversion efficiency. Great efforts have been devoted to chemically engineer $TiO_2$ to reduce its band gap but with only marginal success.[3–7] Although the optical band gap of $TiO_2$ has been successfully reduced, efficient solar conversion devices have not been achieved due to failure in considering other critical solid-state properties for the semiconductor. In most cases, the efforts made toward band gap reduction have been detrimental with regard to other important criteria. For example, monodoping of impurities such as N or C in $TiO_2$ has been applied to reduce the band gap of $TiO_2$. However, the high concentration of these impurities needed for band-gap reduction causes serious carrier recombination and produces inferior-quality materials, making efficient solar-to-hydrogen conversion impossible.

Recent reports have proposed and demonstrated the use of the donor-acceptor codoping concept to improve the solubility of alloying elements and semiconducting material quality.[8–11] However, these reports have only considered low-alloy concentrations and have not taken into account that the band-edge positions and band gaps can change dramatically as the alloying concentration changes. Clearly, a set of rational design strategies are needed such that the proposed methods for engineering potential materials will take all the above criteria into consideration in a collaborative manner. This then can be the pathway to a more rapid discovery of viable semiconductor candidates for PEC.

In this paper, we propose such general design strategies by taking anatase $TiO_2$ as our case study. $TiO_2$ has two material property limitations that must be addressed before it can be considered for solar PEC water splitting. First, as discussed earlier, its band gap is too large for efficient solar light use. Second, its conduction-band minimum (CBM) should be closer to the vacuum level (more negative on the electrochemical scale) to effectively drive the hydrogen reduction reaction. Our approach then must simultaneously lower the band gap, raise the conduction band, and maintain good carrier mobility.

Our strategies include the following: (i) applying donor-acceptor coincorporation to overcome the solubility limits of candidate alloys, reduce recombination, improve material quality, and enhance optical absorption; (ii) using 4*d* and 5*d* cations as donors with higher atomic *d* orbital energies than that of Ti to guarantee that the CBM energy level is not lowered and high electron mobility is maintained; (iii) incorporation of 2*p* or 3*p* anions with higher atomic *p* orbital energies than that of O to raise the valence-band maximum (VBM) to reduce the band gap; and (iv) increase the concentration of the alloying element to improve optical absorption of visible light and hole mobility. We take a two-step approach to determine the best candidates for the donor-acceptor combinations. The first step is to use the calculated atomic orbital trends as rough guidance for rapid screening. The second step is to apply extensive sophisticated density-functional theory (DFT) and well-accepted band-offset calculations to determine the best combinations. We consider donor-acceptor coincorporation at both low and high alloy concentrations. Our results suggest that appropriate donor-acceptor coincorporation of specific elements into anatase $TiO_2$ holds great potential to satisfy all the above criteria simultaneously and therefore may lead to enhanced spontaneous PEC water splitting by sunlight. Nb and Ta, as well as Mo and W, are predicted to be the best choices as donors, and N and C are the best choices as acceptors. The strategies

 

and approaches described here are general and are applicable for searching new materials and engineering other existing materials.

## II. CALCULATION METHODOLOGY

The calculations were performed using DFT as implemented in VASP code using the standard frozen-core projector augmented-wave method.[12,13] For exchange-correlation functional, the generalized gradient approximation (GGA) of Perdew *et al.*[14] was used. The impurity coincorporation was modeled using supercells with randomly distributed impurity pairs. The supercell sizes were allowed to relax. The cutoff energy for basis functions is 350 eV and $k$-point sampling is $7\times7\times3$ for conventional cell of anatase $TiO_2$ and equivalent $k$ points for large supercells.[15] Our calculated lattice parameters for a conventional cell are $a=3.80$ Å, $c=9.65$ Å, and $u=0.207$, which are in very good agreement with experimental values.[16] The band offset was calculated with the commonly used method,[10,11] i.e., the average potentials of host elements far away from impurities are chosen as reference energies in different calculations. The GGA band-gap error was corrected using a scissor operator.

## III. RESULTS AND DISCUSSIONS

The incorporation of a single foreign element can often be limited by the solubility limit in host materials. In the case when high concentration becomes possible, it may create other detrimental issues such as undesirable charged defects, inferior materials quality, and too high carrier concentration. We have previously demonstrated using ZnO as a prototype material that donor-acceptor coincorporation can overcome the solubility limit in a host material, reduce recombination, improve material quality, tune carrier concentration, and enhance optical absorption.[8,9] The passive interaction between a donor and an acceptor, which involves charge transfer between them, is the key. The approach of passivated donor-acceptor coincorporation has also been used by other studies.[10] Therefore, in this work, we will consider only passivated donor-acceptor coincorporation.

For rapid screening of potential donor-acceptor combinations, we first use the calculated atomic-orbital energy levels. Band gaps and band-edge positions of a material are closely connected; the modification of one inevitably alters the other. The VBM of anatase $TiO_2$ is much lower than the $H_2O/O$ redox potential; thus, band-gap reduction in $TiO_2$ should come from introducing occupied bands above the original VBM of $TiO_2$. The VBM of $TiO_2$ is formed by the bonding O $2p$ states; therefore, to upshift the valence-band edge, we need to incorporate anions with $p$ orbital energies higher than that of O $2p$. Figure 1(a) shows our calculated neutral atomic $p$-orbital energy levels for potential anions by the full-electron method with local-density approximation (LDA). The calculated results show that N, C, S, P, Si, Se, As, and Ge can introduce acceptor levels above the VBM of $TiO_2$. For effective alloy incorporation, the size of the element should be as close as possible to the size of the substituted host atom (here, O). Considering the large size difference between P, Si, As, Ge, S, and O, they are excluded from the best choice as acceptors. F, Cl, and Br are also not considered because they are donors at O sites. Therefore, the most appropriate anion alloy elements should be N and C.

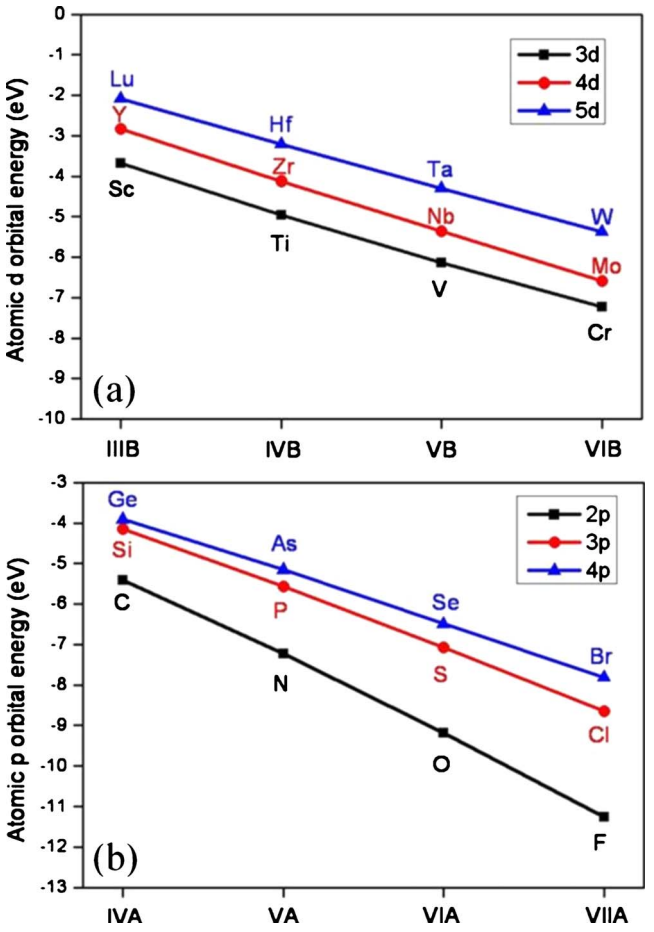


FIG. 1. (Color online) Calculated LDA all-electron atomic-orbital energy levels of neutral atoms studied in this paper. (a) Energy levels for anion $p$ orbitals. (b) Energy levels for cation $d$ orbitals.

The CBM of anatase $TiO_2$ is slightly above the $H_2O/H$ redox potential; thus, any band-gap reduction in $TiO_2$ should maintain the CBM or better upshift the CBM slightly to satisfy the correct band-edge position criterion and provide a slightly higher driving force for hydrogen production. It is known that the CBM of $TiO_2$ is derived mainly from the Ti $3d$ states. Therefore, to maintain or slightly upshift the CBM, the incorporated transition metals (TMs) should have $d$ orbitals with energies higher than that of Ti. Figure 1(b) shows the calculated orbital energy trend for potential neutral TM atoms. For ionized cations (not shown), the energy separation between the $4d$ and $3d$ lines will increase because the $3d$ orbital is more localized. Taking atomic size difference into account, we find that the best choices of dopants for cation site are Ta, Nb, W, and Mo. None of the $3d$ TMs donors (e.g., V and Cr) are on the list because they would introduce new unoccupied bands below the original CBM of $TiO_2$ and possibly shift the conduction-band edge below the $H_2O/H$ redox potential. Furthermore, the localized $3d$ orbit-

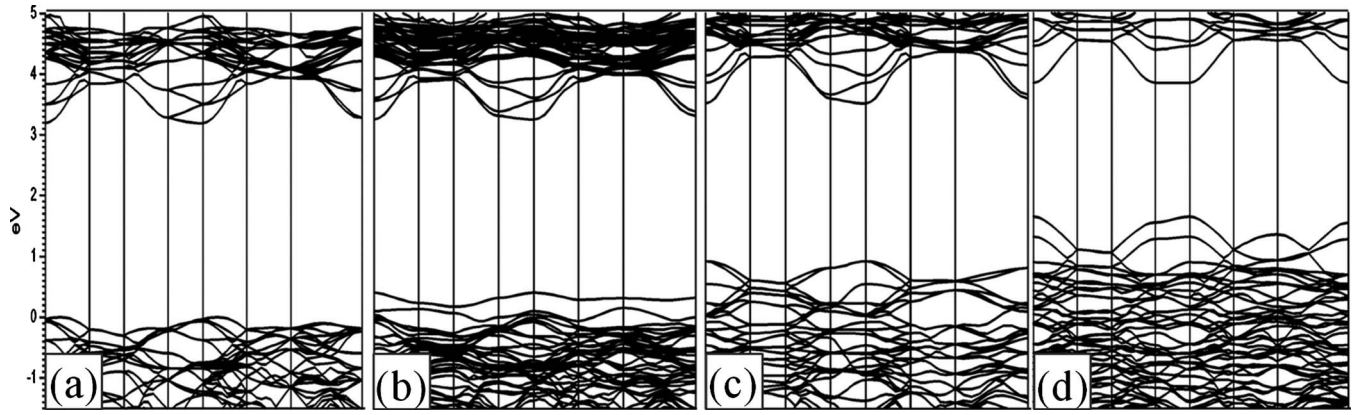


FIG. 2. Calculated GGA band structures for (a) pure $TiO_2$; [(b)–(d)] $TiO_2$ coincorporated with (Ta, N) with different concentrations in which 3.1% O, 12.5% O, and 25% O were replaced by N, respectively. Band offsets are taken into account in these plots.

als will lead to heavy-electron effective mass and low electron mobility.

The above rapid screening process using calculated atomic chemical trends provide quick suggestions for simultaneously satisfying the criteria of band gap and band-edge energetic positions. In the following, we apply this screening process to identify the best alloy combinations by computing the band gaps and band offsets using first-principles band structure calculations. We first consider the (Ta, N) pair because this donor-acceptor pair minimizes the size difference and maximizes the *d* orbital energy differences between the dopant and Ti, and produces the most desirable dispersive acceptor band above the VBM. The calculation is done at a (Ta, N) concentration where 3.1% O is replaced by N. The calculated band structure is shown in Fig. 2(b). Our calculation reveals, as expected from our analysis, that the VBM of the alloyed system is shifted up by 0.34 eV and the conduction band is also *upshifted* by 0.05 eV; thus, the band gap is reduced by 0.29 eV. This reduction is not enough to shift the optical absorption into the optimal visible light regions; for that, we need a band-gap reduction of more than 1 eV.

A commonly used approach to increase the band-gap reduction is to replace N by C, which is on the left-hand side of N in the periodic table; thus, it has a higher *p* orbital energy (see Fig. 1). To passivate the C acceptor, we need to replace Ta by W or Mo. Indeed, our calculation showed that the band-gap reduction is increased to 1.02 eV and 0.83 eV, respectively, for (W, C) and (Mo, C) incorporated systems with the same alloy concentration. The results obtained for the (Mo, C) alloy system is similar to previously calculated results.[10] Unfortunately, these combinations lead to an undesirable downshift of the CBM (see Fig. 4). Moreover, at this low concentration, the defect bands induced by the deep $C_O$ level (C at O site) lead to insufficient optical absorption of visible light and heavy-hole effective mass, and thus, low hole mobility, which are not desirable for efficient PEC.

In this study, we want to emphasize that a better approach to enhance the band-gap reduction is to increase the alloy concentrations. This is because increasing the alloy concentration not only can further reduce the band gap, but can also simultaneously enhance the optical absorption in the long-wavelength regions and reduce the carrier effective mass, all of which are important for an efficient PEC solar conversion material. As an example, our calculated band structures with various (Ta, N) concentrations coincorporated into $TiO_2$ are shown in Fig. 2. The results clearly show that as the concentration increases, the N 2*p* band broadens, the band gap decreases, and the dispersion of the N 2*p* band increases, providing for higher carrier mobility. The GGA calculated band-gap reduction increased to 0.70 eV when 12.5% O is replace by N. Figure 3 shows calculated optical-absorption coefficient spectra for (Ta, N) coincorporated $TiO_2$ with various concentrations. The results show clearly that as the concentration of (Ta, N) pairs increases, the absorption in the longer-wavelength region is dramatically enhanced. The smaller hole effective mass induced by the increased N 2*p* band dispersion at the higher (Ta, N) concentration would lead to higher hole mobility, which is extremely beneficial for improving solar-to-hydrogen conversion efficiency because $TiO_2$ is typically *n* type and a $TiO_2$-based water-splitting device is a minority-carrier device. Most previous calculations have only focused in the low-concentration regime.[10,11] Our results show, however, that there is a strong dependence of the band gap on the alloy concentration. The band-gap reduction predicted at low-alloy concentration may not be applicable to the high-alloy concentration cases. Therefore, to provide a rational prediction of the band gaps

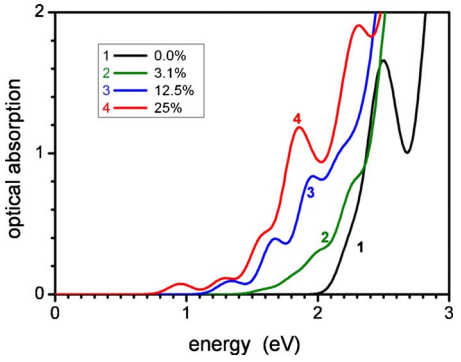


FIG. 3. (Color online) Calculated GGA optical absorption spectra. Spectrum 1 is for pure $TiO_2$. Spectra 2, 3, and 4 are for (Ta, N) coincorporated $TiO_2$ with 3.1%, 12.5%, and 25% of O replaced by N, respectively.

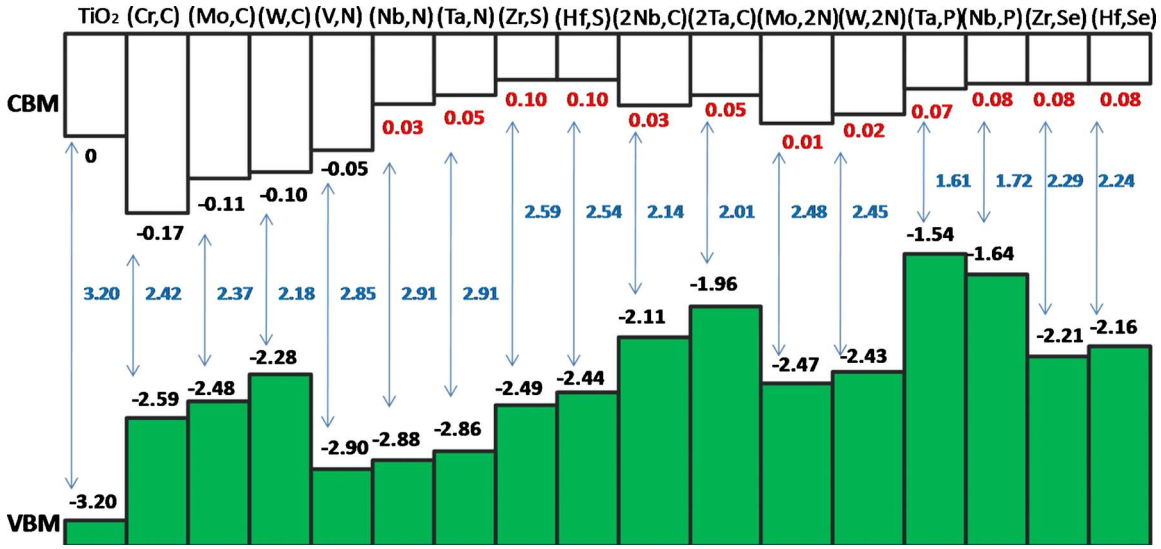


FIG. 4. (Color online) Calculated GGA band offsets (at the Γ point) for $TiO_2$ and $TiO_2$ alloyed with various passivated donor-acceptor combinations in the low-concentration regime. The CBM of pure $TiO_2$ is set to zero as the reference and the band gap is corrected using a scissor operator.

and band-edge positions, the calculations should be conducted at both low- and high-alloy concentrations.

To test the selection of the alloy pair based on the atomic chemical potential, we have performed systematic band structure and band-offset calculations for both low- and high-alloy concentrations. We have considered all possible passivated combinations, such as (one donor, one acceptor), (two donor, one acceptor), and (one donor, two acceptor). In the low-concentration regime, one alloy complex is incorporated in a 48-atom supercell. In this case, 3.1% of O is replaced by acceptors for the (one donor, one acceptor) and (two donor, one acceptor) combinations or 6.25% O is replaced by acceptors for the (one donor, two acceptor) combination. In the high-concentration regime, calculations are performed in a 12-atom supercell containing one alloy complex. Therefore, 12.5% of O is replaced if the complex has one acceptor or 25% O is replaced if it contains two acceptors.

Figure 4 shows the calculated band offsets in the low-concentration regime. The results show that while the incorporation of Ta, Nb, Zr, and Hf as donors can lead to desirable upshifts of the CBM (marked by positive values in Fig. 3), the incorporation of Cr, Mo, W, and V lead to an unwanted downshift of the CBM. The calculated trend for the VBM is consistent with the calculated trend of acceptor atomic-orbital energy levels. For example, the incorporation of P as an acceptor results in the largest upshift of VBM whereas the incorporation of N as an acceptor results in the least upshift of VBM. The band-gap reductions of 1.02 eV and 0.83 eV for (W, C) and (Mo, C) coincorporated systems, respectively, are similar to previously calculated results.[10] The (2Nb, C), (2Ta, C), (Mo, 2N), and (W, 2N) combinations give both better band-gap reduction and band-edge positions. However, the (Mo, 2N) and (W, 2N) combinations are expected to produce more desirable dispersive defect bands. In the low-concentration regime, (Ta, P) and (Nb, P) combinations lead to good band-gap reductions and band-edge energetic positions. The incorporation of S or Se (isovalent to O) can also give good VBM positions and band gaps. However, the large atomic size mismatch between P, S, or Se and O and the localized acceptor defect bands in these systems can have adverse effects on the alloy solubility and carrier transport properties.

At the high donor and acceptor concentration regime, the predicted band gaps and band-edge positions, Fig. 5, change significantly as compared with that in the low-concentration regime. At this high concentration, $TiO_2$ coincorporated with (Cr, C), (Mo, C), (W, C), and (V, N) becomes metallic due to too much band broadening of both unoccupied and occupied bands created by the donors and acceptors. The combinations used to give good band gaps in the low-concentration regime; (2Nb, C), (2Ta, C), (Nb, P), and (Ta, P) now give band gaps that are too narrow due to their high VBM. At this concentration, only the (Nb, N) and (Ta, N) combinations give the desirable band gaps, estimated to be 2.68 eV and 2.50 eV, respectively, with the proper CBM and VBM positions. Our results, therefore, suggest strongly that the band-edge positions and band gaps depend critically on the concentration of the incorporated donors and acceptors pairs. As a general guidance, one must consider carefully band gaps and concentration at the same time so that the appropriate donor-acceptor combinations can be chosen.

It is known that the GGA band structure calculation typically underestimates the band gaps of semiconductors and defect transition energy levels, especially for deep states. This indicates that the GGA-calculated band-gap reduction due to doping could be underestimated. To check the calculation error, we have performed band structure calculations for individual crystal structures using a hybrid density-functional method (HSE),[17] and band-offset calculations with a procedure similar to that used in core-level photoemission measurements.[18] We find that when the total exchange potential contains 22% of the Hartree-Fock exchange potential, the calculated band gap (at the Γ point) for anatase $TiO_2$ is 3.21 eV, which is very close to the experimental value of 3.2 eV.

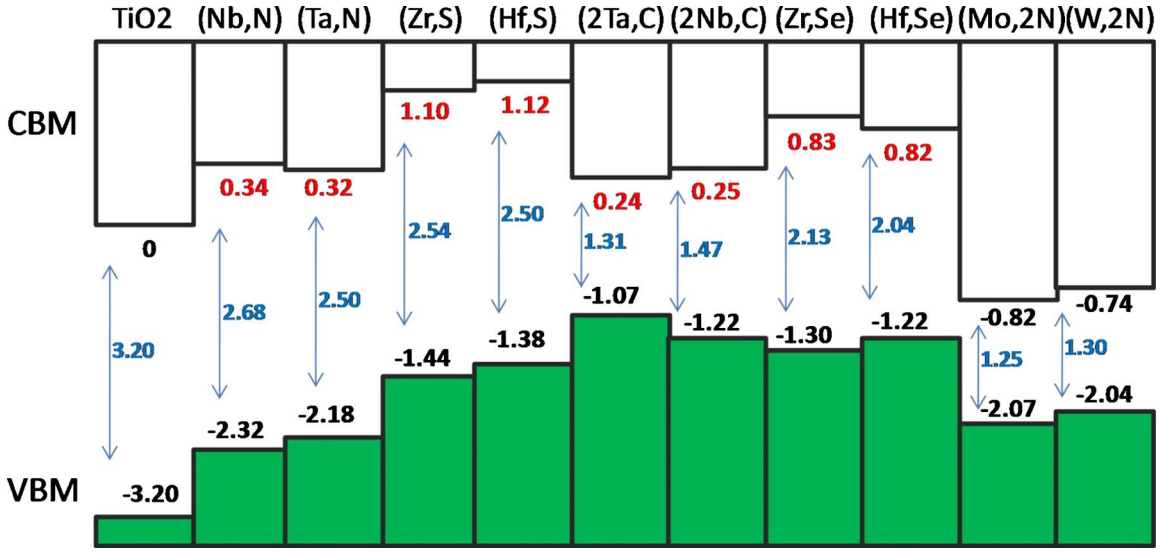


FIG. 5. (Color online) Calculated GGA band offsets (at the Γ point) for $TiO_2$ and $TiO_2$ alloyed with various passivated donor-acceptor combinations in the high-concentration regime. The CBM of pure $TiO_2$ is set to zero as the reference and the band gap is corrected using a scissor operator.

Because of the extensive computing demand, at this time we are only able to calculate the band offsets using the hybrid density-functional method at the high-concentration regime, which can be modeled using a relatively small unit cell. We find that the calculated CBM alignments are very similar for both GGA and HSE hybrid density-functional calculations. However, the upshift of the VBM state calculated by the HSE hybrid functional is about 0.3 eV larger than the GGA results, so the band-gap reduction predicted by the HSE hybrid functional is slightly larger. We would like to point out that the calculated results should only be used as guidance for the trends of band-edge positions and band-gap reductions, rather than an accurate prediction of the band gaps for a particular donor-acceptor coincorporation.

We find that the donor-acceptor pair coincorporation does not cause significant change on the lattice constant. Table I shows the changes in lattice constant for various donor-acceptor pairs in the high-concentration regime. It is seen that even in the high-concentration regime, the changes on lattice constant induced by donor-acceptor pair coincorporation is rather small, which could be the results of optimized size match and strong donor-acceptor interaction. The binding energies of the donor-acceptor combinations provide general guidance on the incorporation ability for these combinations. Our calculated binding energies for donor-acceptor pairs are shown in Table II. The binding energies of codoped $D_{Ti}+A_O$ pairs are calculated by $E_b=E(D_{Ti})+E(A_O)-E(D_{Ti}+A_O)-E_{TiO_2}$, where $E(D_{Ti})$, $E(A_O)$, and $E(D_{Ti}+A_O)$ is the total energy of a supercell with a donor on the Ti site, an acceptor on the O site, and a donor on the Ti site and an acceptor on neighboring O site, respectively. $E_{TiO_2}$ is the total energy of the supercell of pure $TiO_2$. Similar formulas exist for other combinations. We see that most donor-acceptor combinations exhibit very large binding energies. These large binding energies originate from the electron transfer from donor to acceptor and also the Coulomb attractive in-

TABLE I. Changes on lattice constant induced by various donor-acceptor coincorporations in the high-concentration regime.

| Structure | *a* (Å) | *b* (Å) | *c* (Å) |
|---|---|---|---|
| $TiO_2$ | 3.803 | 3.803 | 9.488 |
| $TiO_2$:(Cr, C) | 3.742 | 3.843 | 9.357 |
| $TiO_2$:(Mo, C) | 3.781 | 3.926 | 9.495 |
| $TiO_2$:(Ta, N) | 3.808 | 3.880 | 9.618 |
| $TiO_2$:(Nb, N) | 3.804 | 3.866 | 9.638 |
| $TiO_2$:(Mo, 2N) | 3.925 | 3.776 | 9.438 |

TABLE II. The binding energies (in electron volt) of various donor-acceptor combinations.

| Codoping pair | Binding energy |
|---|---|
| (Cr, C) | 3.02 |
| (Mo, C) | 3.24 |
| (W, C) | 2.86 |
| (V, N) | 2.25 |
| (Nb, N) | 1.97 |
| (Ta, N) | 1.92 |
| (Ta, P) | 0.40 |
| (Nb, P) | 0.58 |
| (Zr, S) | –0.50 |
| (Hf, S) | –0.56 |
| (Zr, Se) | –0.37 |
| (Hf, Se) | –0.44 |
| (2Ta, C) | 1.82 |
| (2Nb, C) | 2.11 |
| (Mo, 2N) | 4.78 |
| (W, 2N) | 4.80 |

teraction between oppositely charged alloy elements. The binding energies for (Ta, P) and (Nb, P) are much smaller than that of other donor-acceptor combinations. This is because the P $3p$ orbital is very high in energy; therefore, the energy gain from charge transfer is significantly less than other donor-acceptor combinations. In addition, the large size difference between P and O causes large lattice distortion. A similar situation exists for doping with Si. The situation is even worse for isovalent defect pairs due to the size mismatch and lack of Coulomb binding. Therefore, using $3p$ elements as a candidate for the acceptor would also face a large challenge on the solubility issue.

## IV. CONCLUSION

In summary, we have proposed general strategies for the rational design of engineering $TiO_2$ to simultaneously meet the criteria required for spontaneous, efficient water splitting by sunlight. We have shown that to achieve high optical absorption of visible light and high carrier mobility, the incorporated donor-acceptor combination must reach a threshold concentration and that the band-gap reduction depends critically on the donor-acceptor concentration. Based on the strategies and extensive DFT band structure calculations, we find that with appropriate donor-acceptor coincorporation alloys with anatase $TiO_2$ hold great potential to simultaneously satisfy all of the PEC water-splitting criteria for high-efficiency solar photoconversion. We predict that (Ta, N) and (Nb, N) pairs are the optimal donor-acceptor combinations in the high-concentration regime, and (Mo, 2N) and (W, 2N) combinations are good candidates in the low-concentration regime for engineering $TiO_2$ to meet band gap, optical absorption, band edge, and mobility criteria. Our design principles are general and can be applicable for searching for other new PEC water-splitting semiconducting materials.

## ACKNOWLEDGMENTS

This work was supported by the U.S. Department of Energy, Hydrogen and Fuel Cells Technology Program. Su-Huai Wei acknowledges support by the Division of Materials Science and Engineering, Office of Basic Energy Sciences.

*Corresponding author; yanfa.yan@nrel.gov

[1] A. Fujishima and K. Honda, Nature (London) **238**, 37 (1972).
[2] M. R. Hoffmann, S. T. Martin, W. Y. Choi, and D. W. Bahnemann, Chem. Rev. **95**, 69 (1995).
[3] X. Chen and S. S. Mao, Chem. Rev. **107**, 2891 (2007).
[4] W. Choi, A. Termin, and M. R. Hoffmann, J. Phys. Chem. **98**, 13669 (1994).
[5] R. Asahi, T. Morikawa, T. Ohwaki, K. Aoki, and Y. Taga, Science **293**, 269 (2001).
[6] K. Nishijima, B. Ohtani, X. L. Yan, T. Kamai, T. Chiyoya, T. Tsubota, N. Murakami, and T. Ohno, Chem. Phys. **339**, 64 (2007).
[7] H. Irie, Y. Watanabe, and K. Hashimoto, Chem. Lett. **32**, 772 (2003).
[8] K.-S. Ahn, Y. Yan, S. Shet, T. Deutsch, J. Turner, and M. Al-Jassim, Appl. Phys. Lett. **91**, 231909 (2007).
[9] S. Shet, K.-S. Ahn, Y. Yan, T. Deutsch, K. M. Chrustowski, J. Turner, M. Al-Jassim, and N. Ravindra, J. Appl. Phys. **103**, 073504 (2008).
[10] Y. Gai, J. Li, S.-S. Li, J. B. Xia, and S.-H. Wei, Phys. Rev. Lett. **102**, 036402 (2009).
[11] W. Zhu, X. F. Qiu, V. Iancu, X.-Q. Chen, H. Pan, W. Wang, N. M. Dimitrijevic, T. Rajh, H. M. Meyer, M. P. Oaranthaman, G. M. Stocks, H. H. Weitering, B. H. Gu, G. Eres, and Z. Y. Zheng, Phys. Rev. Lett. **103**, 226401 (2009).
[12] G. Kresse and J. Furthmuller, Phys. Rev. B **54**, 11169 (1996); Comput. Mater. Sci. **6**, 15 (1996).
[13] P. E. Blöchl, Phys. Rev. B **50**, 17953 (1994); G. Kresse and D. Joubert, *ibid.* **59**, 1758 (1999).
[14] J. P. Perdew and Y. Wang, Phys. Rev. B **45**, 13244 (1992).
[15] H. J. Monkhorst and J. D. Pack, Phys. Rev. B **13**, 5188 (1976).
[16] C. J. Howard, T. M. Sabine, and F. Dickson, Acta Crystallogr., Sect. B: Struct. Sci. **47**, 462 (1991).
[17] J. Heyd, G. E. Scuseria, and M. Ernzerhof, J. Chem. Phys. **118**, 8207 (2003).
[18] S.-H. Wei and A. Zunger, Appl. Phys. Lett. **72**, 2011 (1998).